Revision of the global carbon budget due to changing air-sea oxygen fluxes

Gian-Kasper Plattner,[1] Fortunat Joos, and Thomas F. Stocker

Climate and Environmental Physics, Physics Institute, University of Bern, Switzerland

[1]   Carbon budgets inferred from measurements of the atmospheric oxygen to nitrogen ratio (O_2/N_2) are revised considering sea-to-air fluxes of O_2 and N_2 in response to global warming and volcanic eruptions. Observational estimates of changes in ocean heat content are combined with a model-derived relationship between changes in atmospheric O_2/N_2 due to oceanic outgassing and heat fluxes to estimate ocean O_2 outgassing. The inferred terrestrial carbon sink for the 1990s is reduced by a factor of two compared with the most recent estimate by the Intergovernmental Panel on Climate Change (IPCC). This also improves the agreement between calculated ocean carbon uptake rates and estimates from global carbon cycle models, which indicate a higher ocean carbon uptake during the 1990s than the 1980s. The simulated decrease in oceanic O_2 concentrations is in qualitative agreement with observed trends in oceanic O_2 concentrations.   *INDEX TERMS:* 1635 Global Change: Oceans (4203); 1615 Global Change: Biogeochemical processes (4805); 4806 Oceanography: Biological and Chemical: Carbon cycling; 4805 Oceanography: Biological and Chemical: Biogeochemical cycles (1615); 4842 Oceanography: Biological and Chemical: Modeling; *KEYWORDS:* global carbon budget, changes in ocean heat content, oceanic oxygen outgassing, ocean and land sinks of CO_2, carbon cycle modeling

1.   Introduction

[2]   A quantitative understanding of the carbon cycle is important to develop global warming mitigation strategies. The conventional method, applying an ocean model to estimate the partitioning of anthropogenic carbon between the global terrestrial and ocean carbon sinks [*Siegenthaler and Oeschger*, 1987] has been complemented by various data-based methods to assess the strength of the terrestrial and oceanic carbon sinks [*Keeling et al.*, 1989; *Tans et al.*, 1990; *Keeling and Shertz*, 1992; *Quay et al.*, 1992; *Heimann and Maier-Reimer*, 1996; *Peng et al.*, 1998; *Prentice et al.*, 2001]. Regional estimates of the carbon sinks [e.g., *Enting and Mansbridge*, 1991; *Rayner et al.*, 1999; *Gruber and Keeling*, 2001] are constrained by the global estimates. Here we investigate how global warming and volcanic eruptions affect sea-to-air oxygen (O_2) and nitrogen (N_2) fluxes and, in turn, the carbon budgets for the last 2 decades deduced from the observed trends in atmospheric carbon dioxide (CO_2) and O_2; the latter estimated from measurements of the ratio of oxygen to nitrogen (O_2/N_2) in air [*Keeling et al.*, 1996; *Battle et al.*, 2000; *Manning*, 2001; *Prentice et al.*, 2001].

[3]   The terrestrial and oceanic carbon sinks are estimated by solving the atmospheric budgets of O_2 and CO_2 (Figure 1). The observed increase in atmospheric CO_2 [*Keeling and Whorf*, 2000] equals the known amount of carbon released by fossil fuel burning [*Marland et al.*, 1995] minus the carbon that has been taken up by the ocean and the land biosphere. For each mol CO_2 released by fossil fuel burning, about 1.39 mol O_2 are consumed [*Manning*, 2001]. In turn, about 1.1 mol O_2 are released for each mol CO_2 taken up by the biosphere [*Severinghaus*, 1995], whereas CO_2 uptake by the ocean does not alter atmospheric O_2. The basic assumption has been that sea-to-air O_2 fluxes are negligible on a multiannual timescale, and thus the effect of oceanic O_2 outgassing on the atmospheric O_2 budget has typically been omitted [*Keeling et al.*, 1996; *Bender and Battle*, 1999; *Battle et al.*, 2000] (Figure 1).

[4]   The atmospheric and marine inventories of gaseous or dissolved O_2 are coupled through air-sea gas exchange. O_2 may be released to the atmosphere by a number of processes. First, the solubility of O_2 is reduced in a warming ocean. Second, concentrations of dissolved O_2 are altered by changes in the balance between O_2 transported to depth and O_2 consumed during the remineralization of organic material. A slowed circulation or an increased export production of organic material leads to lower O_2 concentrations at depth and increased O_2 outgassing. And third, increasing storage of organic carbon in dissolved organic matter or in sediments would tend to increase oceanic O_2 inventories. Simulations with coupled atmosphere-ocean biogeochemical models yield a reduced ocean circulation and a decrease in the oceanic O_2 inventory under global warming [*Sar-*
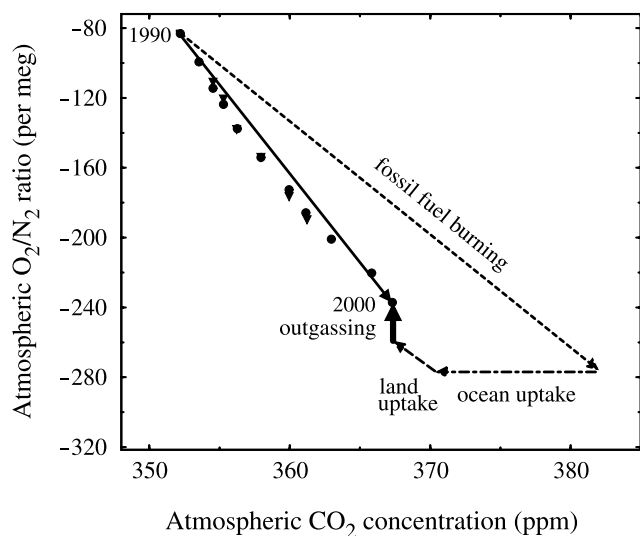
Figure 1. Budgets of atmospheric O_2, expressed as atmospheric O_2/N_2 ratio, and CO_2 (adapted from *Prentice et al.* [2001]). The diagram schematically illustrates the principles of the partitioning of fossil fuel carbon using measurements of atmospheric O_2 and CO_2, by considering simultaneously changes in atmospheric CO_2 (horizontal axis) and O_2 (vertical axis) [*Keeling et al.*, 1996]. The arrow labeled "fossil fuel burning" denotes the effect of the combustion of fossil fuels assuming that 1.39 mol O_2 are consumed for 1 mol CO_2 released [*Manning*, 2001]. The arrow labeled "outgassing" indicates O_2 changes from oceanic outgassing primarily due to changes in the marine biogeochemical cycle; its size is estimated from data of ocean heat uptake [*Levitus et al.*, 2000] and a model-derived relationship between ocean heat fluxes and atmospheric O_2/N_2 changes due to outgassing. Carbon uptake by land and ocean is constrained by the known O_2:CO_2 stoichiometric ratios of these processes [*Severinghaus*, 1995; *Keeling et al.*, 1996; *Battle et al.*, 2000; *Manning*, 2001], defining the slopes of the respective arrows, and the observed changes in atmospheric CO_2 [*Keeling and Whorf*, 2000] and O_2. The trend in atmospheric O_2 is established from measurements of the ratio of O_2 to N_2 in air (solid circles: *Keeling et al.* [1996] and *Manning* [2001]; solid triangles: *Battle et al.* [2000]). Changes in atmospheric O_2/N_2 are usually given in units of per meg. A per meg corresponds to a relative difference in the O_2/N_2 ratio of two samples of 10^{-6} [*Keeling et al.*, 1996].

miento et al., 1998; *Matear et al.*, 2000; *Plattner et al.*, 2001; R. J. Matear and A. C. Hirst, Predicted ocean outgassing of oxygen and nitrogen with climate change: Implications for carbon budgeting, submitted to *Geochemical Geophysical Geosystems*, 2002.]. (Hereinafter referred to as Matear and Hirst, submitted manuscript, 2002.)

[5] In an earlier model study, we showed that global warming induced O_2 outgassing should be taken into account when estimating the carbon sinks from atmospheric O_2/N_2 observations and that the global sink flux of carbon into the terrestrial biosphere is potentially overestimated by about half a Gt C yr^{-1} in recent carbon budgets [*Plattner et al.*, 2001]. However, the impacts of internal climate variability,

explosive volcanic eruptions, and changes in solar irradiance on O_2 outgassing have been neglected. Recently, *Keeling and Garcia* [2002], analyzing oceanic observations of dissolved O_2 and temperature, and *Bopp et al.* [2002], applying a coupled atmosphere-ocean biogeochemical model, have estimated the oceanic O_2 outgassing and revised the O_2/N_2-based carbon budgets for recent decades.

[6] Here we build on our previous work and investigate further how global warming and natural climate variability affect sea-to-air O_2 fluxes by applying a physical-biogeochemical climate model. The impacts of explosive volcanic eruptions and changes in solar irradiance are explicitly considered. The carbon budgets of the Intergovernmental Panel on Climate Change (IPCC) for the 1980s and 1990s [*Prentice et al.*, 2001; *Manning*, 2001] are revised. This is done by combining the model-derived relationship between changes in atmospheric O_2/N_2 from oceanic outgassing and ocean heat uptake with observations of changes in ocean heat content [*Levitus et al.*, 2000]. In this way, we account for decadal scale climate variability reflected in the ocean heat content data, but not readily simulated for a particular decade.

2. Model and Methods

[7] We have used a low-order physical-biogeochemical climate model that consists of a zonally averaged ocean model, coupled to an atmospheric energy balance model [*Stocker et al.*, 1992] including an active hydrological cycle [*Schmittner and Stocker*, 1999], and a representation of the carbon cycle in the ocean [*Marchal et al.*, 1998] and the terrestrial biosphere [*Siegenthaler and Oeschger*, 1987]. Model configuration and spin-up to a modern steady state are as given by *Plattner et al.* [2001], except that vertical resolution in the upper 1,000 m has been increased to 20 levels. This has little impact on simulated distributions of dissolved O_2 and other tracers and does not alter the conclusions. Nitrogen (N_2) was added as an inorganic tracer to simulate solubility driven changes in N_2 sea-to-air fluxes. The O_2 air-sea gas exchange is now explicitly considered in the model. Air-sea gas exchange of O_2 and N_2 is dependent on windspeed and temperature [*Wanninkhof*, 1992]. Details on the incorporation of O_2 and N_2 in the physical-biogeochemical climate model and on the different model simulations performed are provided in the Appendix.

[8] Radiative forcing from reconstructed (until year 2000) and later projected changes in the abundances of greenhouse gases and aerosols in the atmosphere was calculated based on simplified expressions [see *Joos et al.*, 2001, and references therein]. We consider radiative forcing from changes in atmospheric CO_2, CH_4, N_2O, stratospheric and tropospheric O_3, stratospheric H_2O due to CH_4 changes, SF_6, 28 halocarbons (including those controlled by the Montreal Protocol), from direct and indirect effects of sulfate aerosols, and from direct forcing of black and organic carbon. Radiative forcing by explosive volcanic eruptions and solar irradiance changes was prescribed for the last millennium [*Crowley*, 2000]. Transient runs start at year 1000 A. D. Output is only analyzed after 1400 A. D. to exclude the transition into a slightly different ocean circulation state after addition of radiative forcing by

Table 1. Carbon Uptake Rates by the Ocean and by the Terrestrial Biosphere[a]

Carbon Fluxes, GtC yr^{-1}	From Atmospheric O_2/N_2		From Ocean Models	
	IPCC[b]	Revised[c]	This Study[d]	OCMIP Models[e]
Period 1980–1989				
Ocean-atmosphere flux	−1.9 ± 0.6	−1.7 ± 0.6	−1.9	−1.9 (1.5 − 2.1)
Land-atmosphere flux	−0.2 ± 0.7	−0.4 ± 0.7		
Period 1990–1999				
Ocean-atmosphere flux	−1.7 ± 0.5	−2.4 ± 0.7	−2.2	−2.0 (1.7 − 2.3)
Land-atmosphere flux	−1.4 ± 0.7	−0.7 ± 0.8		
Difference Between the 2 Decades (1990s Minus 1980s)				
Ocean-atmosphere flux	+0.2	−0.7	−0.3	−0.1
Land-atmosphere flux	−1.2	−0.3		

[a] Positive values are fluxes to the atmosphere; negative values represent uptake from the atmosphere. Error ranges denote uncertainty (one standard deviation), not interannual variability, which is substantially larger.
[b] Based on intradecadal trends in atmospheric CO_2 and O_2 as given by the IPCC [*Prentice et al.*, 2001] and detailed by *Manning* [2001]. A small correction for solubility driven O_2 outgassing is included.
[c] Corrected for the effect of oceanic O_2 outgassing caused by changes in the marine biogeochemical cycles. The correction is estimated from data of ocean heat uptake [*Levitus et al.*, 2000] and the model-derived linear relationship between ocean heat uptake rates and changes in atmospheric O_2/N_2 due to outgassing (1.56 per meg/10^{22} J).
[d] Ocean carbon uptake rates calculated by prescribing annual-mean atmospheric CO_2 from observations at Mauna Loa and South Pole [*Keeling and Whorf*, 2000] in the standard model setup.
[e] Ocean carbon uptake rates averaged from simulations of eight models participating in the Ocean Carbon-Cycle Model Intercomparison Project (OCMIP) (adapted from *Orr* [2000]); model range is given in parentheses. Global warming feedbacks are not considered in the OCMIP simulations. Prescribed atmospheric CO_2 is higher than observed during the 1990s in the OCMIP simulations; the ocean carbon uptake rates shown have been obtained by scaling the original OCMIP results downward by 13%, based on the baseline simulation and the OCMIP simulation with our model.

volcanoes; the North Atlantic Deep Water formation rate dropped from 22 to 18 Sv (1 Sv = 10^6 m^3 s^{-1}). The model's climate sensitivity, that is the increase in global mean surface air temperature for a doubling of atmospheric CO_2, $\Delta T_{2\times}$, was set to 3.7°C in the standard simulation and 0°C in the baseline simulation (constant climate and ocean circulation).

[9] The model has been tested by various oceanic tracers [*Marchal et al.*, 1998], applied in paleoclimate and global warming studies [e.g., *Stocker and Schmittner*, 1997; *Marchal et al.*, 1999; *Plattner et al.*, 2001], and evaluated within the Ocean Carbon-Cycle Model Intercomparison Project (OCMIP) [*Orr*, 2000; *Dutay et al.*, 2002]. Modeled oceanic CO_2 uptake rates for the 1980s and 1990s are well within current data based estimates (Table 1). Integrated ocean CO_2 uptake over the industrial period and the 21st century is reduced by about 8% in simulations with global warming as compared to simulations without global warming [*Joos et al.*, 1999b; *Plattner et al.*, 2001], consistent with other studies investigating the feedbacks between global warming and the ocean carbon cycle [*Prentice et al.*, 2001]. The modeled rate of North Atlantic Deep Water formation decreases only slightly during the industrial period in the standard simulation (about 1.7 Sv). The simulated surface warming during the last century of 0.51°C is comparable to the observed warming of 0.6 ± 0.2°C [*Jones et al.*, 1999].

3. Results
3.1. Modeled Air-Sea Fluxes of O_2 and Heat

[10] The ocean is taking up heat in response to greenhouse gas forcing (Figure 2). The increasing trend in modeled ocean heat content is temporarily reversed in the years after explosive volcanic eruptions (Figure 3a). The modeled change in oceanic heat content between 1955 and 1995 is in close agreement with observations [*Levitus et al.*, 2000]. However, similar to studies applying coupled atmosphere-ocean general circulation models [e.g., *Barnett et al.*, 2001; *Levitus et al.*, 2001; *Bopp et al.*, 2002], decadal scale variability in the ocean heat content is substantially underestimated. The observed decadal scale variations stem mainly from the Pacific Ocean [*Levitus et al.*, 2000] and may be due to internal climate oscillations such as El Niño/Southern Oscillation or the Pacific Decadal Oscillation that are not resolved in our model.
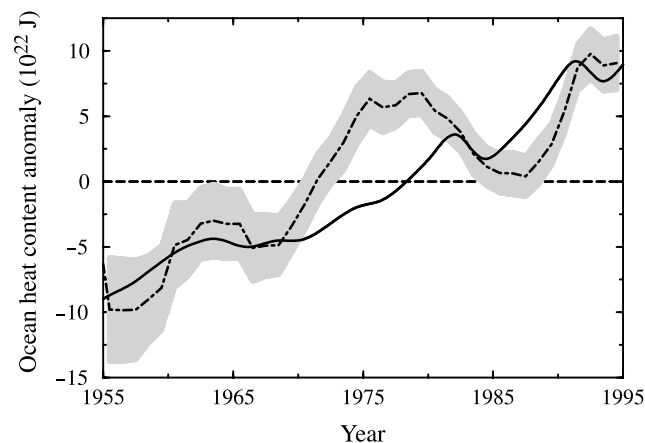

Figure 2. Ocean heat content anomaly versus time. Observed (dash-dotted line; *Levitus et al.* [2000]) and modeled (solid line; $\Delta T_{2\times}$ = 3.7°C) oceanic heat content anomalies during the last 5 decades. Data and model results are 5-year running means relative to the average for the 40-year period. Uncertainties (1 standard deviation) in observations are indicated by the shaded band.
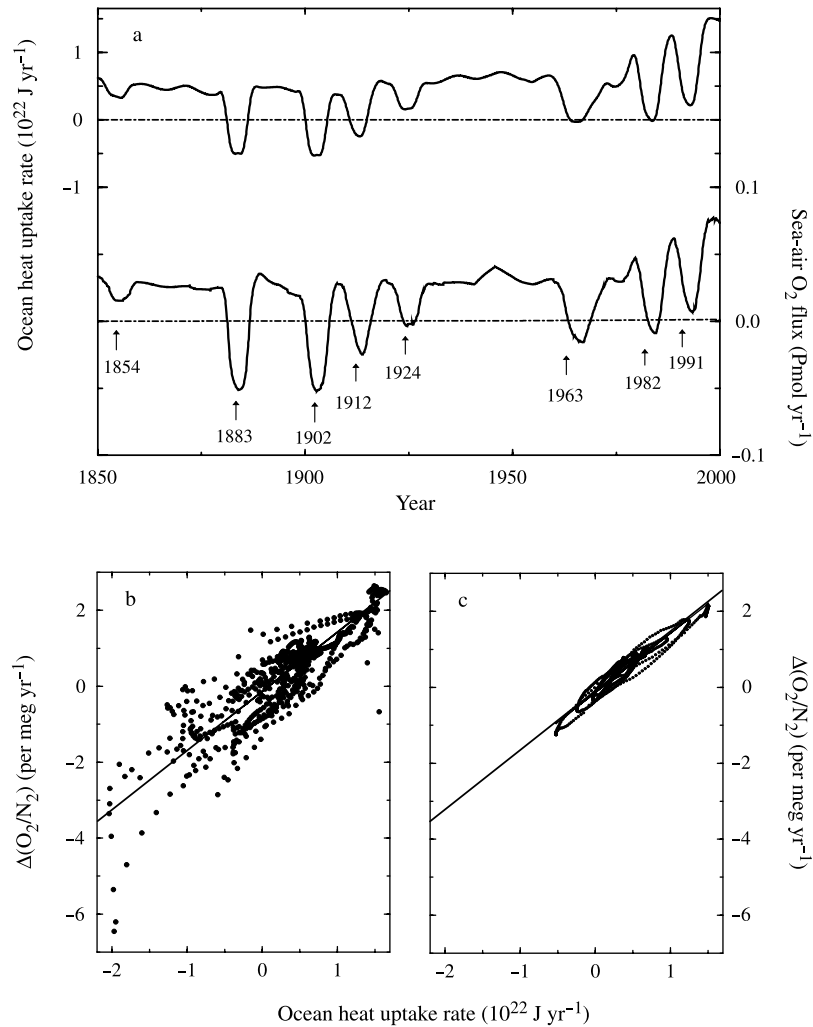
Figure 3. Simulated ocean heat uptake and O_2 outgassing. (a) Modeled ocean heat uptake rates and modeled sea-to-air O_2 fluxes from the standard simulation ($\Delta T_{2\times} = 3.7°C$) for the period 1850 to 2000; results are smoothed by 5-year running means. Modeled fluxes from the baseline simulation ($\Delta T_{2\times} = 0°C$) are given by dashed lines. Major volcanic eruptions are indicated by arrows. (b and c) Modeled change in atmospheric O_2/N_2 from air-sea gas exchange, $\Delta(O_2/N_2)$, versus modeled heat uptake rates (1900 to 2000) for monthly values (Figure 3b) and their 5-year running means (Figure 3c). $\Delta(O_2/N_2)$ is calculated as the difference between monthly changes in O_2/N_2 from the standard ($\Delta T_{2\times} = 3.7°C$) and the baseline simulation ($\Delta T_{2\times} = 0°C$) (see Appendix A2). Both, smoothed and unsmoothed monthly values show a strong linear relationship. The slope of the regression (solid line) is 1.56 per meg/10^{22} J for the smoothed model results ($r^2 = 0.94$).

[11] Related to the slow warming, there is a net flux of O_2 from the ocean to the atmosphere over the industrial period (Figure 3a). The modeled long-term trend in the sea-to-air flux is interrupted following explosive volcanic eruptions that cause short-term oceanic O_2 uptake. The sea-to-air fluxes of O_2 and N_2 alter atmospheric O_2/N_2 by about 12.3 per meg during the 1990s in the standard simulation. This corresponds to 30% of the difference between the observed decrease in atmospheric O_2 and the amount of O_2 consumed by fossil fuel burning (Figure 1). This difference is conventionally attributed to O_2 release from the land biosphere associated with carbon uptake. Hence, the terrestrial carbon sink would also be reduced by 30% when considering modeled oceanic O_2 outgassing.

3.2. Revision of the Carbon Budget

[12] The close correlation between ocean heat uptake and changes in atmospheric O_2/N_2 from oceanic outgassing (Figures 3b and 3c) suggests that observations of changes in ocean heat content [*Levitus et al.*, 2000] can be utilized to estimate the O_2 outgassing and to revise the recent carbon budget published by the Intergovernmental Panel on Climate Change (IPCC) [*Prentice et al.*, 2001; *Manning*, 2001] (Table 1). Thereby we attempt to account for internal climate variability not readily reproduced by our model

for individual decades. Simulated sea-to-air O_2 fluxes and ocean heat uptake rates are tightly correlated on multiannual to multidecadal timescales (Figure 3a). A change in ocean heat uptake of 10^{22} J corresponds to an increase in atmospheric O_2/N_2 of 1.56 per meg when correlating ($r^2 = 0.94$) simulated heat fluxes and associated O_2/N_2 changes over the period 1900 to 2000 (Figures 3b and 3c). We combine this relation with data-based estimates of ocean heat uptake [*Levitus et al.*, 2000] and atmospheric O_2/N_2 and CO_2 [*Manning*, 2001; *Prentice et al.*, 2001]. Observed trends in the oceanic heat content are $-0.39 \cdot 10^{22}$ J yr^{-1} for the 1980s and $+1.24 \cdot 10^{22}$ J yr^{-1} for the period 1990 to 1995. The available ocean heat content data are extrapolated to the year 2000 assuming the same annual heat uptake rate ($+1.24 \cdot 10^{22}$ J yr^{-1}) as during 1990 to 1995. This assumption appears to be supported by data of the heat content anomaly of the ocean's uppermost 300 m [*Levitus et al.*, 2000] (see section 3.4).

[13] This new approach yields rates of carbon uptake by the terrestrial biosphere that are slightly higher during the 1980s and a factor of 2 lower during the 1990s than the central estimates published by the IPCC [*Prentice et al.*, 2001]. As a result, oceanic CO_2 uptake rates are now found to be higher during the 1990s than the 1980s in contrast to the central estimates of the IPCC, although uncertainties in the carbon budget do not allow to determine a reliable trend in the carbon sinks (Table 1). An increase in ocean CO_2 uptake over the last two decades is in agreement with estimates derived from ocean models [*Orr*, 2000] (Table 1) and from observations of the $^{13}C/^{12}C$ ratio of atmospheric CO_2 [*Joos et al.*, 1999a; *Keeling et al.*, 2001].

3.3. Uncertainties in the Budget Revision

[14] Uncertainties in the estimated sinks of anthropogenic CO_2 due to uncertainties in the atmospheric trends of O_2/N_2 and CO_2, fossil fuel emissions, and the stoichiometric relation between CO_2 released and O_2 consumed during fossil fuel burning and terrestrial carbon release, are taken from *Prentice et al.* [2001] (Table 1). Uncertainties in the correction of the carbon sinks arise from uncertainties in the observed ocean heat uptake [*Levitus et al.*, 2000] and in the model-derived relationship between heat uptake rates and atmospheric O_2/N_2 changes due to oceanic outgassing.

[15] The robustness of the model-derived relationship has been tested by varying key physical and biogeochemical parameters of the model and the applied radiative forcing (Appendix, Tables A1 and A2). For vertical diffusivity, governing the strength of the thermohaline overturning [*Wright and Stocker*, 1992] and vertical mixing of O_2 and heat, set to 0.2 or $0.6 \cdot 10^{-4}$ m^2 s^{-1} (standard: $0.4 \cdot 10^{-4}$ m^2 s^{-1}) the estimated correction in the carbon sinks is 25% smaller or 31% larger than in the standard simulation. Changes in biological export production, parameterized in the model as a function of dissolved inorganic phosphate, affect dissolved O_2, but not heat uptake. A simulation was performed where the export production was kept constant. Then, the correction is 6% larger than in the standard simulation, where the export production is slightly reduced. Applying a stoichiometric ratio of O_2:P of -138 in the organic matter cycle (Redfield ratio), results in a 15%

smaller correction compared to the standard run, where O_2:P was set to -170. A smaller O_2:P Redfield ratio implies less formation of dissolved O_2 during organic matter production and less O_2 consumption during remineralization.

[16] A different temporal evolution and different types of external forcing affect ocean heat uptake and O_2 outgassing differently. Simulations were performed with the climate sensitivity set to 1.5 or 5.0°C, with anthropogenic forcing only, with volcanic forcing only, with volcanic and solar forcing combined, with indirect aerosol forcing neglected or doubled. For all these cases the estimated correction in the carbon sinks varies by less than ±16% around the standard value of 0.246 Gt C yr^{-1} for the 1980s and 0.778 Gt C yr^{-1} for the 1990s (Appendix, Table A1). However, when the correlation was evaluated over the periods 1800 to 2100, 2000 to 2100, or 2100 to 2500 for different emission scenarios [*Nakićenović et al.*, 2000], and different CO_2 stabilization profiles [*Schimel et al.*, 1997; *Wigley et al.*, 1997], the correction was about halved compared to the standard case (Appendix, Table A2). This suggests that the O_2 to heat flux ratio may decrease in the future.

[17] Overall, the uncertainty in the correction due to uncertainties in the model-derived relationship between heat uptake rates and O_2/N_2 changes due to outgassing is estimated to be around 30% based on these additional simulations where model parameters and forcing were varied. This corresponds to uncertainties in the corrections of ±0.1 Gt C yr^{-1} for the 1980s and ±0.2 Gt C yr^{-1} for the 1990s.

[18] The uncertainty in the correction of the carbon sinks due to uncertainty in the ocean heat content data for the 1980s is estimated to be ±0.2 Gt C yr^{-1} by combining the errors in the observed heat content anomaly at the beginning and the end of the decade [*Levitus et al.*, 2000] and assuming them to be independent. Heat uptake rates during the 1990s are estimated to be uncertain by a factor of two due to the data extrapolation for the period 1995 to 2000; this alone yields an uncertainty in the correction of ±0.4 Gt C yr^{-1}.

[19] Combined uncertainties are calculated by gaussian error propagation. This yields a total correction of the carbon sinks of 0.25 ± 0.22 Gt C yr^{-1} for the 1980s and of 0.78 ± 0.44 Gt C yr^{-1} for the 1990s. This correction is applied to the carbon budgets of the IPCC for the 1980s and 1990s [*Prentice et al.*, 2001; *Manning*, 2001] (Table 1). Then, best estimates and uncertainties of the revised CO_2 uptake rates by the terrestrial biosphere are 0.4 ± 0.7 Gt C yr^{-1} for the 1980s and 0.7 ± 0.8 Gt C yr^{-1} for the 1990s (Table 1).

3.4. An Alternative Scenario for Ocean Heat Uptake

[20] We have additionally applied an alternative scenario for ocean heat uptake to further investigate the robustness of our approach. Observations of the heat content anomaly for the uppermost 300 m of the ocean are used instead for the uppermost 3000 m. Heat data for the top 300 m are available as annual values until 1998, whereas the available heat data for the top 3000 m are 5-year running mean values that are only available until 1995 [*Levitus et al.*, 2000]. Besides this difference in the applied heat data, the same
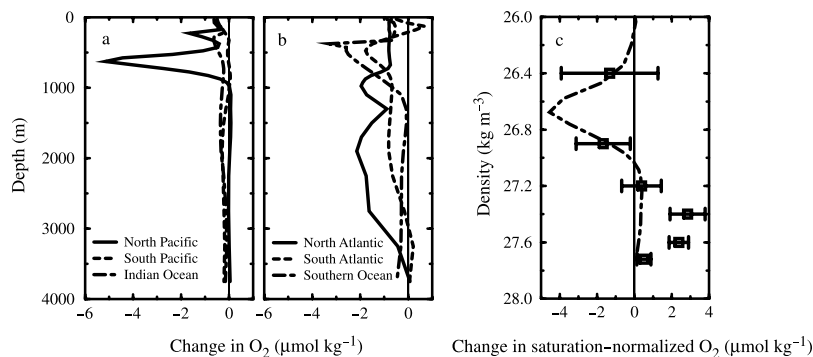
Figure 4. Depth profiles of changes in dissolved O_2. Modeled basin-average changes in dissolved O_2 versus depth for (a) the North Pacific (solid line), the South Pacific (dashed line), the Indian (dash-dotted line), and (b) the North Atlantic (solid line), South Atlantic (dashed line), and the Southern Ocean (south of 47.5°S; dash-dotted line). Results are differences between decadal-mean O_2 concentrations for the 1970s and 1990s. Modeled ocean-mean concentration of dissolved O_2 decreased by 0.414 μmol kg^{-1} during this period. All results are for the standard model setup. (c) Observed (squares; *Keller et al.* [2002]) and modeled (dot-dashed) basin-average changes (1970s to 1990s) in saturation-normalized dissolved O_2 averaged for water masses of equal density (referenced to surface pressure) between 300 and 2500 m in the North Pacific. Error bars indicate uncertainties (1 standard deviation) in observations.

method as described in section 3.2 is used to determine the correction of the carbon budget.

[21] Observed trends in the oceanic heat content of the uppermost 300 m are $-0.16 \cdot 10^{22}$ J yr^{-1} for the 1980s and $+0.67 \cdot 10^{22}$ J yr^{-1} for the period 1990 to 1998. The uppermost 300 m of the World Oceans exhibit a strong warming after year 1995. Simulated changes in the oceanic heat content of the top 300 m are tightly correlated on multiannual to multidecadal timescales with simulated changes in atmospheric O_2/N_2 due to outgassing. A change in heat content of the top 300 m of 10^{22} J corresponds to an increase in atmospheric O_2/N_2 of 2.25 per meg ($r^2 = 0.81$, period 1900 to 2000) for the standard model setup. The heat content anomaly for the uppermost 300 m of the ocean is extrapolated for the year 1999 assuming the same annual change in heat content ($+0.67 \cdot 10^{22}$ J yr^{-1}) as during 1990 to 1998. The deduced corrections in the terrestrial carbon sink are $+0.15$ Gt C yr^{-1} for the 1980s and -0.60 Gt C yr^{-1} for the 1990s. These values are smaller than the corrections obtained from the top 3000 m heat data, but still within the uncertainties of the corrections provided above. Thus, the 300 m heat data support our extrapolation of the trend in total ocean heat uptake for the second half of the 1990s, that was used to revise the carbon budget in section 3.2. Data-based estimates of oceanic heat content anomaly for the entire ocean and the period 1995 to 2000 will probably become available in the near future. This will provide a better basis for the estimated correction in the carbon budget.

3.5. Modeled Versus Observed Changes in Oceanic Dissolved O_2

[22] The simulated oceanic O_2 concentration changes are small and roughly consistent with previous results based on oceanic observations. Modeled basin-average changes (1970s to 1990s) are less than 5 μmol kg^{-1}, and largest changes are found in the upper 1000 m in the Pacific, South Atlantic, Indian, and Southern Oceans, and below 1500 m in the North Atlantic (Figures 4a and 4b). Such small long-term changes are difficult to detect from observations. Interpolation of sparse data may introduce biases. Cruises at different times may yield different results due to natural variability, changes in water masses, or intercruise calibration differences. To account for these effects, analyses are usually performed for saturation-normalized O_2 concentrations on density surfaces, and intercruise deep-water concentration differences are assumed to reflect calibration differences.

[23] Modeled saturation-normalized O_2 concentrations are averaged on density surfaces (referenced to surface pressure) and compared to previous results based on oceanic observations for the North Pacific. Saturation-normalized O_2 decreased by up to 5 μmol kg^{-1} in the upper ocean, and increased slightly below 1000 m (Figure 4c). The simulated changes in the upper water column and below 2000 m are consistent with the O_2 changes estimated by *Keller et al.* [2002] for the entire North Pacific, analyzing O_2 measurements from the 1970s and 1990s. However, O_2 changes between 1000 and 2000 m are smaller in the model than estimated by *Keller et al.* [2002].

[24] Modeled trends in O_2 concentrations are generally less than 1 μmol kg^{-1} per decade in all basins. Larger changes are simulated only in the top 1000 m in the circumpolar region (reductions up to 5 μmol kg^{-1} per decade) and in the northernmost grid cells in the Atlantic and Pacific Oceans which exhibit marked changes in convection resulting in zonally averaged O_2 reductions of up to 16 μmol kg^{-1} per decade. The simulated changes in the zonally averaged model are qualitatively comparable to large local changes observed in the circumpolar region [*Matear et al.*, 2000], in middle and high latitudes of the North Pacific region [*Emerson et al.*, 2001; *Kim et al.*, 2000; *Ono et al.*, 2001; *Watanabe et al.*, 2001], in the South Pacific [*Shaffer et al.*, 2000], in the Indian Ocean [*Bindoff and McDougall*, 2000], and in the North Atlantic [*Garcia et al.*, 1998; *Garcia and Keeling*, 2001].

[25] *Matear et al.* [2000] found reductions in dissolved O_2 of up to 6 μmol kg^{-1} per decade in the circumpolar region (53°S – 61°S; 110°E – 160°E) by analyzing data from the recent World Ocean Circulation Experiment (WOCE) and from the 1968 Eltanin cruise. It is an open question whether this decrease is representative for the entire Southern Ocean. *Emerson et al.* [2001] found local reductions in saturation-normalized O_2 of up to 30 μmol kg^{-1} in data from cruises in the 1980s and 1990s along 150°W in the North Pacific. A large O_2 decrease is also found in available long-term studies. *Kim et al.* [2000] report large long-term decreases in oceanic O_2 concentrations of more than 20 μmol kg^{-1} mainly below 1000 m in the East Sea (Japan Sea) since the mid-1950s and of nearly 10 μmol kg^{-1} since 1979. *Ono et al.* [2001] and *Watanabe et al.* [2001] found a reduction in dissolved oxygen of up to 30 μmol kg^{-1} superimposed on a bidecadal oscillation in subsurface waters in the western subarctic Pacific (Oyashio domain) over the period from 1968 to 1998. *Shaffer et al.* [2000] report decreases of dissolved O_2 above 3000 m at 28°S in the eastern South Pacific off Chile (72°W – 88°W) since 1967, ranging from about 18 μmol kg^{-1} at 300 m to about 4 μmol kg^{-1} at 2000 m. *Bindoff and McDougall* [2000] observed a pronounced decrease in O_2 concentrations of 7 to 8 μmol kg^{-1} between 300 and 1000 m depth occurring at 32°S in the Indian Ocean (averaged from 30°E – 117°E) over the period 1962 to 1987. Finally, *Garcia et al.* [1998] found a significant decrease in O_2 concentration between 700 and 1800 m at 24°N in the North Atlantic over the period 1981 to 1992. The zonally averaged decrease in the O_2 concentration is between 3 and 7 μmol kg^{-1}, with the maximum occurring around 1100 m.

[26] In summary, detectable decreases in O_2 have been observed in intermediate waters in the North Pacific, North Atlantic, South Pacific, and South Indian Oceans, and small increases have occurred in deeper waters in the North Pacific and South Indian Oceans [*Keeling and Garcia*, 2002]. These observations support the simulated long-term decrease in the oceanic O_2 inventory.

3.6. Mechanisms Driving the Modeled Changes in Dissolved O_2

[27] Finally, we examine the mechanisms responsible for the changes in the modeled oceanic O_2 concentrations. Two additional model simulations were performed to quantify the contribution of different mechanisms to changes in O_2 concentrations. In a first simulation, sea surface temperatures and salinities from the standard simulation ($\Delta T_{2\times} = 3.7$°C) were prescribed in the routines to calculate solubilities of O_2 and N_2, while running the model in the constant-climate baseline setup ($\Delta T_{2\times} = 0$°C) up to year 2000. In a second simulation, the biological export production was kept constant, while otherwise the configuration was identical to the standard simulation. The main cause for the reduction in dissolved O_2 and the increase in the net sea-to-air O_2 flux in the standard simulation is a reduction in the transport rate of O_2 to depth due to changes in ocean circulation and convection. This is also supported by various studies that identify ocean circulation changes as the main cause of observed O_2 reductions [*Emerson et al.*, 2001; *Keller et al.*, 2002; *Kim et al.*, 2000; *Watanabe et al.*,

2001; *Ono et al.*, 2001; *Shaffer et al.*, 2000; *Bindoff and McDougall*, 2000]. The small reduction in simulated biological export production in the standard run tends to slightly increase the marine O_2 inventory and to reduce outgassing. Solubility changes, mainly driven by sea surface warming, are responsible for about 22% of the simulated reduction in the marine oxygen inventory, but for only about 10% of the changes in atmospheric O_2/N_2 as the solubility of both O_2 and N_2 is reduced. This highlights the importance of ocean circulation changes for atmospheric O_2/N_2.

4. Discussion and Conclusion

[28] Data-based and model studies suggest that the oceanic O_2 inventory has decreased over the past decades. In our standard global warming simulation, the oceanic O_2 inventory decreases by $0.42 \cdot 10^{14}$ mol yr^{-1} over the 1990s, well within the range of 0.2 to $0.7 \cdot 10^{14}$ mol yr^{-1} found by others [*Sarmiento et al.*, 1998; *Matear et al.*, 2000; *Plattner et al.*, 2001; *Bopp et al.*, 2002; *Keeling and Garcia*, 2002; Matear and Hirst, submitted manuscript, 2002]. As discussed in section 3.5, a long-term decrease in dissolved O_2 concentration is observed in different oceanic regions.

[29] A close relationship between sea-to-air oxygen fluxes and heat fluxes is found in many modeling studies [*Sarmiento et al.*, 1998; *Plattner et al.*, 2001; *Bopp et al.*, 2002] as well as in a data-based study [*Keeling and Garcia*, 2002]. The ratios between O_2 to heat flux and N_2 to heat flux are 5.9 nmol J^{-1} and 2.1 nmol J^{-1} over the period 1900 to 2000 in our standard simulation. This compares well with O_2 to heat flux ratios of about 6 nmol J^{-1} found in simulations with increasing atmospheric CO_2 [*Sarmiento et al.*, 1998; *Bopp et al.*, 2002] and of 5 nmol J^{-1} derived from oceanic temperature and dissolved O_2 observations [*Keeling and Garcia*, 2002]. *Keeling and Garcia* [2002] also report a comparable N_2 to heat flux ratio (2.2 nmol J^{-1}). Sensitivity simulations (Appendix, Table A1) suggest that the O_2 to heat flux ratio over the industrial period is relatively insensitive to variations in model parameters and to variations in radiative forcing. However, future scenario simulations (Appendix, Table A2) show that the O_2 to heat flux ratio is likely to decrease in the coming decades.

[30] Corrections of the recent carbon budget of the IPCC [*Prentice et al.*, 2001] are suggested in three independently developed studies. Similar to this study, *Keeling and Garcia* [2002] and *Bopp et al.* [2002] combine estimates of the O_2 to heat flux ratio with estimates of ocean heat uptake to compute sea-to-air O_2 fluxes and revise carbon budgets. Similar values of the O_2 to heat flux ratio are applied. However, the three studies differ fundamentally in the way ocean heat uptake is considered. *Keeling and Garcia* [2002] applied a model-derived estimate of the long-term ocean warming trend [*Levitus et al.*, 2001; *Barnett et al.*, 2001] and neglected decadal scale variability in heat uptake. On the other hand, ocean heat content data of *Levitus et al.* [2000] are used here and in the study of *Bopp et al.* [2002], assuming that O_2 outgassing is related to both the long-term warming trend and the decadal scale variability. The analysis by *Bopp et al.* [2002] of decadal scale variations in their model and our sensitivity simulation where the model is

driven by the pulse-like volcanic forcing only (Appendix, Table A1) suggest that O_2 outgassing is coupled to decadal scale variations in heat uptake.

[31] The two different approaches yield different corrections for the carbon budget due to O_2 outgassing. The consideration of long-term warming only yields a small upward revision in ocean carbon uptake of +0.2 Gt C yr^{-1} as suggested by *Keeling and Garcia* [2002]. This correction would apply for both the 1980s and 1990s. Consideration of the large decadal variability in the heat anomaly data yields a substantial upward revision of ocean carbon uptake for the 1990s, but a small negative correction for the 1980s. *Bopp et al.* [2002] estimated a correction in the ocean carbon sink of +0.5 ± 0.5 Gt C yr^{-1} for the period 1990 to 1996 and of −0.1 ± 0.5 Gt C yr^{-1} for the 1980s comparable to our estimates of +0.7 ± 0.5 Gt C yr^{-1} and −0.2 ± 0.3 Gt C yr^{-1}.

[32] In conclusion, oceanic O_2 changes need to be considered to determine a self-consistent estimate of the terrestrial and oceanic sinks of anthropogenic CO_2 from atmospheric O_2/N_2 observations. We propose to monitor trends in dissolved O_2 by routine measurements from ships or buoys to further narrow uncertainties in estimates of the carbon sinks and to resolve the discrepancies between the different studies discussed above.

[33] Estimates of the oceanic carbon sink obtained by different approaches [*Prentice et al.*, 2001; *Orr*, 2000; *Joos et al.*, 1999a; *Keeling et al.*, 2001; *Rayner et al.*, 1999] are consistent when taking into account their uncertainties. However, the central estimates of the IPCC budget show a lower oceanic carbon uptake during the 1990s than the 1980s in contrast to results from process-based carbon cycle models and estimates based on measurements of the $^{13}C/^{12}C$ ratio of atmospheric CO_2. The consideration of oceanic O_2 outgassing reconciles the central estimates from atmospheric O_2/N_2 data with results from ocean models and analyses of carbon isotopes.

[34] Our results suggest that the global net carbon uptake by the land biosphere during the 1990s was about a factor of two lower than that recently estimated by the IPCC [*Prentice et al.*, 2001]. This is of relevance as the performance of process-based carbon cycle models is evaluated against the recent carbon budget [*McGuire et al.*, 2001; *Orr et al.*, 2001].

Appendix A
A1. Implementation of the Biogeochemical Cycles of O_2 and N_2 in the Model

[35] The atmospheric budget equations for O_2 and N_2 are included in the model by

$$\frac{\partial I_{atm}^{O_2}}{\partial t} = -F_{air-sea}^{O_2} - 1.39 \cdot F_{fossil}^C + 1.1 \cdot F_{air-biota}^C \quad (A1)$$

and

$$\frac{\partial I_{atm}^{N_2}}{\partial t} = -F_{air-sea}^{N_2}, \quad (A2)$$

where $I_{atm}^{O_2}$ and $I_{atm}^{N_2}$ are the atmospheric inventories of O_2 and N_2, and $F_{air-sea}^{O_2}$ and $F_{air-sea}^{N_2}$ are the net air-to-sea gas exchange of O_2 and N_2. F_{fossil}^C denotes the carbon emissions from fossil fuel burning and $F_{air-biota}^C$ the net atmosphere to

land biota flux of CO_2. The fossil fuel $O_2:CO_2$ combustion ratio of −1.39 and the land biota $O_2:CO_2$ exchange ratio of −1.1 are taken from *Manning* [2001] and *Severinghaus* [1995], respectively. O_2 and N_2 are allowed to evolve freely in the atmosphere after being initialized by prescribing the preindustrial mole fractions of O_2 and N_2 in the atmosphere. Preindustrial atmospheric mole fractions of O_2 and N_2 are set to 209,460 ppm and 780,840 ppm [see *Manning et al.*, 1999, and references therein]. All inventories, concentrations and fluxes are expressed in molar units in the model.

[36] $F_{air-biota}^C$ is the sum of the CO_2 flux from deforestation and land-use change, F_{defor}^C, and the modeled CO_2 flux into the terrestrial biosphere due to fertilization, F_{fert}^C:

$$F_{air-biota}^C = F_{fert}^C - F_{defor}^C. \quad (A3)$$

[37] F_{defor}^C is calculated by closing the atmospheric CO_2 budget (single deconvolution [*Siegenthaler and Oeschger*, 1987]) from prescribed atmospheric CO_2 [*Keeling and Whorf*, 2000] and fossil fuel emissions [*Marland et al.*, 1995], and from the modeled fertilization flux, F_{fert}^C, and CO_2 air-sea gas exchange, $F_{air-sea}^C$:

$$F_{defor}^C = \frac{\partial I_{atm}^C}{\partial t} - F_{fossil}^C + F_{air-sea}^C + F_{fert}^C. \quad (A4)$$

[38] The net air-sea fluxes of O_2 and N_2 are calculated as the product of the gas transfer coefficient, k_g, and the partial pressure difference between surface air and water:

$$F_{air-sea}^{\mathcal{T}} = k_g(p\mathcal{T}_{sat} - p\mathcal{T}_w) = k_w([\mathcal{T}_{sat}] - [\mathcal{T}_w]), \quad (A5)$$

where the terms $p\mathcal{T}_{sat}$ and $p\mathcal{T}_w$ denote the saturation and the modeled partial pressures of a tracer $\mathcal{T}$ in seawater. The partial pressures of O_2 and N_2 in seawater are calculated from the concentrations of dissolved O_2 and N_2 in seawater ($[\mathcal{T}_{sat}]$ and $[\mathcal{T}_w]$) and the solubilities of *Weiss* [1970]. The coefficient k_g equals the product of the solubility [*Weiss*, 1970] and the gas transfer velocity related to the liquid phase, k_w. k_w is calculated applying the formulation of *Wanninkhof* [1992] for long-term winds and a wind speed climatology [*Esbensen and Kushnir*, 1981]. Results obtained by applying equation A5 are nearly identical to results obtained assuming dissolution equilibrium with atmospheric O_2 [*Plattner et al.*, 2001] as the equilibration time of the ocean mixed layer with O_2 is short (about 20 days) [*Broecker and Peng*, 1982].

[39] Tracers are implemented in the ocean as described by *Marchal et al.* [1998]. The conservation equations for O_2 and N_2 are

$$\frac{\partial \mathcal{T}_{oce}}{\partial t} = -\mathbf{u} \cdot \nabla \mathcal{T}_{oce} + \nabla \cdot (\kappa \nabla \mathcal{T}_{oce}) + q_{conv}^{\mathcal{T}} + J_{bio}^{\mathcal{T}} + J_{flux}^{\mathcal{T}}, \quad (A6)$$

where $\mathcal{T}_{oce}$ is the tracer concentration in the ocean. The first term on the right describes advective transport (with the velocity vector $\mathbf{u}$), the second term on the right describes diffusive transport (with the the diffusion tensor κ), and $q_{conv}^{\mathcal{T}}$ denotes the transport by convection. The terms $J_{bio}^{\mathcal{T}}$ and

Table A1. Ratio of $\Delta(O_2/N_2)$ to Heat Flux: Sensitivity on Model Parameters and Radiative Forcing[a]

	Period 1990–1999	
Model Setup	$\Delta(O_2/N_2)$/Heat Flux [per meg/10^{22} J]	r^2. 1
Standard		
$\Delta T_{2\times} = 3.7°C$, standard simulation	1.56(—)	0.95
Climate Sensitivity, $\Delta T_{2\times}$		
$\Delta T_{2\times} = 1.5°C$	1.43(−9%)	0.90
$\Delta T_{2\times} = 5.0°C$	1.55(−1%)	0.95
Radiative Forcing and Climate Sensitivity, $\Delta T_{2\times}$		
$\Delta T_{2\times} = 3.7°C$, anthropogenic forcing only	1.46(−6%)	0.98
$\Delta T_{2\times} = 1.5°C$, anthropogenic forcing only	1.73(−11%)	0.98
$\Delta T_{2\times} = 5.0°C$, anthropogenic forcing only	1.36(−13%)	0.98
$\Delta T_{2\times} = 3.7°C$, volcanic forcing only	1.80(+16%)	0.92
$\Delta T_{2\times} = 3.7°C$, volcanic and solar forcing only	1.77(+14%)	0.89
$\Delta T_{2\times} = 3.7°C$, no indirect aerosol forcing	1.51(−3%)	0.98
$\Delta T_{2\times} = 3.7°C$, doubled indirect aerosol forcing	1.65(+6%)	0.95
$\Delta T_{2\times} = 3.7°C$, anthropogenic forcing only, starting 1765	1.46(−6%)	0.98
$\Delta T_{2\times} = 3.7°C$, scenario WRE starting 1765, CO_2 forcing only	1.17(−25%)	0.90
Marine Biology		
$\Delta T_{2\times} = 3.7°C$, constant export production	1.65(+6%)	0.94
$\Delta T_{2\times} = 3.7°C$, stoichiometric ratio O_2:P set to −138	1.33(−15%)	0.95
Ocean Circulation and Mixing		
$\Delta T_{2\times} = 3.7°C$, vertical diffusivity $0.2 \cdot 10^{-4}$ m^2 s^{-1}	1.18(−25%)	0.92
$\Delta T_{2\times} = 3.7°C$, vertical diffusivity $0.6 \cdot 10^{-4}$ m^2 s^{-1}	2.03(+31%)	0.87

[a] The model-derived relationship between heat uptake rates and O_2/N_2 changes due to outgassing is calculated from model output (5-year running means) of the period 1900 to 2000. The relationship is given in per meg/10^{22} J for each individual simulation and additionally as %-difference (in parentheses) from the ratio of $\Delta(O_2/N_2)$ to heat flux obtained from the standard simulation. The resulting correction in the carbon budget scales linearly with the $\Delta(O_2/N_2)$ to heat flux ratio. The term r^2 denotes the coefficient of determination for each individual correlation.

J_{flux}^T represent source minus sink terms due to biological processes and air-sea fluxes. The term J_{bio}^T is zero for N_2 and the total inventory of N_2 in the atmosphere-ocean system is conserved.

A2. Computing the Correction of the Carbon Budget

[40] Changes in the modeled atmospheric O_2/N_2 ratio are expressed relative to the preindustrial ratio in units of per meg according to *Keeling et al.* [1996]:

$$\delta(O_2/N_2) = [(O_2/N_2)/(O_2/N_2)_{ref} - 1] \cdot 10^6. \quad (A7)$$

Normalization to N_2 eliminates variations associated with changes in humidity and other atmospheric changes unrelated to O_2 and CO_2 fluxes [*Bender and Battle*, 1999].

[41] The change in atmospheric O_2/N_2 from air-sea gas exchange (in per meg yr^{-1}), $\Delta(O_2/N_2)$, is calculated as the difference between changes in O_2/N_2 from the standard simulation ($\Delta T_{2\times} = 3.7°C$) and the baseline simulation ($\Delta T_{2\times} = 0°C$):

$$\Delta(O_2/N_2) = \delta(O_2/N_2)_{std} - \delta(O_2/N_2)_{base}. \quad (A8)$$

[42] Simulated $\Delta(O_2/N_2)$ and simulated heat fluxes are correlated to compute the ratio between atmospheric O_2/N_2 changes due to outgassing and ocean heat uptake (see Figures 3b and 3c). Then, observed changes in ocean heat content [*Levitus et al.*, 2000] are multiplied by this model-derived ratio to estimate the change in atmospheric O_2/N_2

due to ocean outgassing, $\Delta(O_2/N_2)*$, for the 1980s and 1990s. By considering $\Delta(O_2/N_2)*$ instead of the modeled $\Delta(O_2/N_2)$, we account for decadal scale climate variability reflected in the ocean heat data, but not readily simulated for a particular decade.

[43] The correction in the terrestrial and oceanic carbon sinks (in Gt C yr^{-1}) is then obtained by

$$\Delta F_{air-biota}^C = -\Delta F_{air-sea}^C = -\frac{1}{2.49} \cdot \Delta(O_2/N_2)*. \quad (A9)$$

The factor $-\frac{1}{2.49}$ arises from the conversion of per meg O_2/N_2 to gigatons of carbon [*Battle et al.*, 2000].

A3. Sensitivity and Scenario Simulations

[44] Uncertainties in the correction of the carbon sinks arise from uncertainties in the model-derived relationship between heat uptake rates and O_2/N_2 changes due to outgassing. The robustness of this relationship has been tested by varying key physical and biogeochemical parameters of the model, the applied radiative forcing, and the period over which model output has been used to derive the relationship.

[45] In Table A1, results from sensitivity simulations on model parameters and on the applied radiative forcing are shown. The model-derived relationship is calculated from 5-year running mean model output of the period 1900 to 2000. Using 1-year running mean or monthly-mean values does not alter results significantly. The calculated slope for the

Table A2. Ratio of $\Delta(O_2/N_2)$ to Heat Flux: Sensitivity on the Period Used to Derive the Relationship Between Heat Uptake Rates and O_2/N_2 Changes due to Outgassing[a]

	Period 1990 – 1999	
Model setup	$\Delta(O_2/N_2)$/heat flux [per meg/10^{22} J]	r^2 [1]
Period 1400–2000		
$\Delta T_{2\times} = 3.7°C$, standard simulation	1.63(+5%)	0.96
$\Delta T_{2\times} = 3.7°C$, volcanic forcing only	1.72(+10%)	0.93
$\Delta T_{2\times} = 3.7°C$, volcanic solar forcing only	1.73(+11%)	0.93
Period 1800–2100		
$\Delta T_{2\times} = 3.7°C$, anthropogenic forcing only	0.98(−37%)	0.98
$\Delta T_{2\times} = 1.5°C$, anthropogenic forcing only	1.12(−28%)	0.97
$\Delta T_{2\times} = 5.0°C$, anthropogenic forcing only	0.89(−43%)	0.98
$\Delta T_{2\times} = 3.7°C$, scenario B1 starting 1765, anthropogenic forcing only	0.98(−38%)	0.98
$\Delta T_{2\times} = 3.7°C$, scenario A1FI starting 1765, anthropogenic forcing only	0.77(−51%)	0.97
$\Delta T_{2\times} = 3.7°C$, scenario WRE550 starting 1765, CO_2 forcing only	0.93(−40%)	0.97
$\Delta T_{2\times} = 3.7°C$, scenario WRE1000 starting 1765, CO_2 forcing only	0.86(−45%)	0.97
Period 2000–2100		
$\Delta T_{2\times} = 3.7°C$, anthropogenic forcing only	0.78(−50%)	0.94
$\Delta T_{2\times} = 1.5°C$, anthropogenic forcing only	0.64(−59%)	0.88
$\Delta T_{2\times} = 5.0°C$, anthropogenic forcing only	0.65(−58%)	0.96
$\Delta T_{2\times} = 3.7°C$, scenario B1 starting 1765, anthropogenic forcing only	0.78(−50%)	0.93
$\Delta T_{2\times} = 3.7°C$, scenario A1FI starting 1765, anthropogenic forcing only	0.62(−60%)	0.97
Period 2100–2500		
$\Delta T_{2\times} = 3.7°C$, scenario WRE550 starting 1765, CO_2 forcing only	0.94(−40%)	0.88
$\Delta T_{2\times} = 3.7°C$, scenario WRE1000 starting 1765, CO_2 forcing only	0.73(−53%)	0.46

[a] The model-derived relationship between heat uptake rates and O_2/N_2 changes due to outgassing is calculated from model output (5-year running means) of the periods 1400 to 2000, 1800 to 2100, 2000 to 2100, and 2100 to 2500. The relationship is given in per meg/10^{22} J for each individual simulation and additionally as %-difference (in parentheses) from the ratio of $\Delta(O_2/N_2)$ to heat flux obtained from the standard simulation (see Table A1). The resulting correction in the carbon budget scales linearly with the $\Delta(O_2/N_2)$ to heat flux ratio. The term r^2 denotes the coefficient of determination for each individual correlation.

standard model setup is reduced from 1.56 per meg/10^{22} J ($r^2 = 0.94$) to 1.51 per meg/10^{22} J ($r^2 = 0.86$; 1-year running means) or 1.50 per meg/10^{22} J ($r^2 = 0.80$; monthly means), respectively. We note that the resulting correction in the carbon budget scales linearly with the $\Delta(O_2/N_2)$ to heat flux ratio.

1. Climate sensitivity: The climate sensitivity, $\Delta T_{2\times}$, in the standard simulation set to 3.7°C, has been varied between 1.5 and 5.0°C.

2. Radiative forcing: In the standard simulation radiative forcing from reconstructed (until year 2000) and later projected changes in the abundances of greenhouse gases and aerosols in the atmosphere was calculated based on simplified expressions [see *Joos et al.*, 2001, and references therein]. The radiative forcing from changes in atmospheric CO_2, CH_4, N_2O, stratospheric and tropospheric O_3, stratospheric H_2O due to CH_4 changes, SF_6, 28 halocarbons (including those controlled by the Montreal Protocol), from direct and indirect effects of sulfate aerosols, and from direct forcing of black and organic carbon has been considered. Radiative forcing by explosive volcanic eruptions and solar irradiance changes was prescribed for the last millennium [*Crowley*, 2000]. Additional simulations have been performed where the applied radiative forcing has been varied between anthropogenic forcing only, volcanic forcing only, volcanic and solar forcing only, and with the indirect aerosol forcing excluded or doubled.

3. Marine biology: Two additional simulations were performed to test the sensitivity on parameters of the biogeochemical model. In the first simulation the export production was kept constant. In the second simulation a stoichiometric ratio of O_2:P of −138 in the organic matter cycle (Redfield ratio) has been applied instead of −170 as in the standard.

4. Ocean circulation and mixing: The vertical diffusivity, governing the strength of the thermohaline overturning [*Wright and Stocker*, 1992] and vertical mixing of O_2 and heat, has been varied between 0.2 and $0.6 \cdot 10^{-4}$ m^2 s^{-1}. In the standard simulation it is set to $0.4 \cdot 10^{-4}$ m^2 s^{-1}.

[46] In Table A2, results from sensitivity and scenario simulations are listed. The model-derived relationship between ocean heat uptake rates and O_2/N_2 changes due to outgassing is calculated using model output (5-year running means) from the periods 1400 to 2000, 1800 to 2100, 2000 to 2100, and 2100 to 2500, in contrast to Table A1 where model output from the period 1900 to 2000 is used. Future emissions of CO_2, non-CO_2 greenhouse gases and aerosols are prescribed from the IPCC SRES emission scenarios [*Nakićenović et al.*, 2000] or the WRE CO_2 stabilization profiles [*Schimel et al.*, 1997; *Wigley et al.*, 1997].

References

Barnett, T. R., D. W. Pierce, and R. Schnur, Detection of anthropogenic climate changes in the World's oceans, *Science*, 292, 270–274, 2001.

Battle, M., M. L. Bender, P. P. Tans, J. M. C. White, J. T. Ellis, T. Conway, and R. J. Francey, Global carbon sinks and their variability inferred from atmospheric CO_2 and ^{13}C, *Science*, 287, 2467–2470, 2000.

Bender, M., and M. Battle, Carbon cycle studies based on the distribution of O_2 in air, *Tellus, Ser. B*, 51, 165–169, 1999.

Bindoff, N. L., and T. J. McDougall, Decadal changes along an Indian Ocean section at 32°S and their interpretation, *J. Phys. Oceanogr.*, 30, 1207–1222, 2000.

Bopp, L., C. Le Quéré, M. Heimann, A. C. Manning, and P. Monfray, Climate-induced oceanic oxygen fluxes: Implications for the contemporary carbon budget, *Global Biogeochem. Cycles*, 16, 1022, doi:10.1029/2001GB001445, 2002.

Broecker, W. S., and T.-H. Peng, *Tracers in the Sea*, Lamont-Doherty Earth Obs., Palisades, N. Y., 690 pp., 1982.

Crowley, T., Causes of climate change over the past 1000 years, *Science*, 289, 270–277, 2000.

Dutay, J.-C., et al., Evaluation of ocean model ventilation with CFC-11: Comparison of 13 global ocean models, *Ocean Modell.*, 4, 98–120, 2002.

Emerson, S., S. Mecking, and J. Abell, The biological pump in the subtropical North Pacific Ocean: Nutrient sources, Redfield ratios, and recent changes, *Global Biogeochem. Cycles*, 15, 535–554, 2001.

Enting, I. G., and J. V. Mansbridge, Latitudinal distribution of sources and sinks of CO_2: Results of an inversion study, *Tellus, Ser. B*, 43, 156–170, 1991.

Esbensen, S. K., and V. Kushnir, The heat budget of the global ocean: An atlas based on estimates from surface marine observations, *Tech. Rep. 29*, Clim. Res. Inst., Oreg. State Univ., Corvallis, 1981.

Garcia, H., and R. F. Keeling, On the global oxygen anomaly and air-sea flux, *J. Geophys. Res.*, 106, 31,155–31,166, 2001.

Garcia, H., A. Cruzado, L. Gordon, and J. Escanez, Decadal-scale chemical variability in the subtropical North Atlantic deduced from nutrient and oxygen data, *J. Geophys. Res.*, 103, 2817–2830, 1998.

Gruber, N., and C. D. Keeling, An improved estimate of the isotopic air-sea disequilibrium of CO_2: Implications for the oceanic uptake of anthropogenic CO_2, *Geophys. Res. Lett.*, 28, 555–558, 2001.

Heimann, M., and E. Maier-Reimer, On the relations between the oceanic uptake of CO_2 and its carbon isotopes, *Global Biogeochem. Cycles*, 10, 89–110, 1996.

Jones, P. D., M. New, D. E. Parker, S. Martin, and I. G. Rigor, Surface air temperature and its changes over the past 150 years, *Rev. Geophys.*, 37, 173–199, 1999.

Joos, F., R. Meyer, M. Bruno, and M. Leuenberger, The variability in the carbon sinks as reconstructed for the last 1000 years, *Geophys. Res. Lett.*, 26, 1437–1440, 1999a.

Joos, F., G.-K. Plattner, T. F. Stocker, O. Marchal, and A. Schmittner, Global warming and marine carbon cycle feedbacks on future atmospheric CO_2, *Science*, 284, 464–467, 1999b.

Joos, F., I. C. Prentice, S. Sitch, R. Meyer, G. Hooss, G.-K. Plattner, S. Gerber, and K. Hasselmann, Global warming feedbacks on terrestrial carbon uptake under the IPCC emission scenarios, *Global Biogeochem. Cycles*, 15, 891–907, 2001.

Keeling, C. D., and T. P. Whorf, Atmospheric CO_2 records from sites in the SIO air sampling network, in *Trends: A Compendium of Data on Global Change*, Carbon Dioxide Inf. Anal. Cent., Oak Ridge Natl. Lab., Oak Ridge, Tenn., 2000.

Keeling, C. D., R. B. Bacastow, A. F. Carter, S. C. Piper, T. P. Whorf, M. Heimann, W. G. Mook, and H. Roeloffzen, A three-dimensional model of atmospheric CO_2 transport based on observed winds, 1, Analysis of observational data, in *Aspects of Climate Variability in the Pacific and the Western Americas*, *Geophys. Monogr. Ser.*, vol. 55, edited by D. H. Peterson, pp. 165–236, AGU, Washington, D. C., 1989.

Keeling, C. D., S. C. Piper, R. B. Bacastow, M. Wahlen, T. P. Whorf, M. Heimann, and H. A. Meijer, Exchanges of atmospheric CO_2 and $^{13}CO_2$ with the terrestrial biosphere and oceans from 1978 to 2000, I, *Tech. Rep. SIO Ref. Ser. 01–06*, Scripps Inst. of Oceanogr., San Diego, Calif., 2001.

Keeling, R. F., and H. Garcia, The change in oceanic O_2 inventory associated with recent global warming, *Proc. Natl. Acad. Sci. USA*, 99, 7848–7853, 2002.

Keeling, R. F., and S. R. Shertz, Seasonal and interannual variations in atmospheric oxygen and implications for the global carbon cycle, *Nature*, 358, 723–727, 1992.

Keeling, R. F., S. C. Piper, and M. Heimann, Global and hemispheric CO_2 sinks deduced from changes in atmospheric O_2 concentrations, *Nature*, 381, 218–221, 1996.

Keller, K., R. D. Slater, M. Bender, and R. M. Key, Possible biological or physical explanations for decadal scale trends in North Pacific nutrient concentrations and oxygen utilization, *Deep Sea Res., Part II*, 49, 345–362, 2002.

Kim, K.-R., K. Kim, D.-J. Kang, S. Y. Park, M.-K. Park, Y.-G. Kim, H. S. Min, and D. Min, The East Sea (Japan Sea) in change: A story of dissolved oxygen, *Mar. Technol. Soc. J.*, 33, 15–22, 2000.

Levitus, S., J. I. Antonov, T. P. Boyer, and C. Stephens, Warming of the World Ocean, *Science*, 287, 2225–2229, 2000.

Levitus, S., J. I. Antonov, J. Wang, T. L. Delworth, K. W. Dixon, and A. J. Broccoli, Anthropogenic warming of Earth's climate system, *Science*, 292, 267–270, 2001.

Manning, A. C., Temporal variability of atmospheric oxygen from both continuous measurements and a flask sampling network: Tools for studying the global carbon cycle, Ph.D. thesis, 190 pp., Univ. of Calif., San Diego, La Jolla, 2001.

Manning, A. C., R. F. Keeling, and J. P. Severinghaus, Precise atmospheric oxygen measurements with a paramagnetic oxygen analyzer, *Global Biogeochem. Cycles*, 13, 1107–1115, 1999.

Marchal, O., T. F. Stocker, and F. Joos, A latitude-depth, circulation-biogeochemical ocean model for paleoclimate studies: Model development and sensitivities, *Tellus, Ser. B*, 50, 290–316, 1998.

Marchal, O., T. F. Stocker, F. Joos, A. Indermühle, T. Blunier, and J. Tschumi, Modelling the concentration of atmospheric CO_2 during the Younger Dryas climate event, *Clim. Dyn.*, 15, 341–354, 1999.

Marland, G., T. A. Boden, and R. J. Andres, Global, regional and national annual CO_2 emission estimates from fossil-fuel burning, hydraulic-cement production and gas flaring: 1950 to 1992, *Carbon Dioxide Inf. Anal. Cent. Commun. Fall*, 20–21, 1995.

Matear, R. J., A. C. Hirst, and B. I. McNeil, Changes in dissolved oxygen in the Southern Ocean with climate change, *Geochem. Geophys. Geosyst.*, 1, Paper number 2000GC000086, 2000.

McGuire, A. D., et al., Carbon balance of the terrestrial biosphere in the twentieth century: Analyses of CO_2, climate and land-use effects with four process-based ecosystem models, *Global Biogeochem. Cycles*, 15, 186–206, 2001.

Nakićenović, N., et al., *Special Report on Emission Scenarios*, 599 pp., Intergov. Panel on Clim. Change, Cambridge Univ. Press, New York, 2000.

Ono, T., T. Midorikawa, Y. W. Watanabe, K. Tadokoro, and T. Saino, Temporal increases of phosphate and apparent oxygen utilization in the subsurface waters of western subarctic Pacific from 1968 to 1998, *Geophys. Res. Lett.*, 28, 3285–3288, 2001.

Orr, J. C., OCMIP carbon analysis gets underway, *Res. GAIM*, 3(2), 4–5, 2000.

Orr, J. C., et al., Estimates of anthropogenic carbon uptake from four three-dimensional global ocean models, *Global Biogeochem. Cycles*, 15, 43–60, 2001.

Peng, T.-H., R. Wanninkhof, J. L. Bullister, R. A. Feely, and T. Takahashi, Quantification of decadal anthropogenic CO_2 uptake in the ocean based on dissolved inorganic carbon measurements, *Nature*, 396, 560–563, 1998.

Plattner, G.-K., F. Joos, T. F. Stocker, and O. Marchal, Feedback mechanisms and sensitivities of ocean carbon uptake under global warming, *Tellus, Ser. B*, 53, 564–592, 2001.

Prentice, I. C., G. D. Farquhar, M. J. R. Fasham, M. L. Goulden, M. Heimann, V. J. Jaramillo, H. S. Kheshgi, C. Le Quéré, R. J. Scholes, and D. W. R. Wallace, The carbon cycle and atmospheric carbon dioxide, in *Climate Change 2001: The Scientific Basis: Contribution of Working Group I to the Third Assessment Report of the Intergovernmental Panel on Climate Change*, edited by J. T. Houghton et al., 881 pp., Cambridge Univ. Press, New York, 2001.

Quay, P. D., B. Tilbrook, and C. S. Wong, Oceanic uptake of fossil fuel CO_2: Carbon-13 evidence, *Science*, 256, 74–79, 1992.

Rayner, P. J., I. G. Enting, R. J. Francey, and R. Langenfelds, Reconstructing the recent carbon cycle from atmospheric CO_2, $\delta^{13}C$ and O_2/N_2 observations, *Tellus, Ser. B*, 51, 213–232, 1999.

Sarmiento, J. L., T. M. C. Hughes, R. J. Stouffer, and S. Manabe, Simulated response of the ocean carbon cycle to anthropogenic climate warming, *Nature*, 393, 245–249, 1998.

Schimel, D., M. Grubb, F. Joos, R. Kaufmann, R. Moos, W. Ogana, R. Richels, and T. Wigley, Stabilisation of atmospheric greenhouse gases: Physical, biological, and socio-economic implications, *Tech. Pap. III*, 48 pp., Intergov. Panel on Clim. Change, Geneva, 1997.

Schmittner, A., and T. F. Stocker, The stability of the thermohaline circulation in global warming experiments, *J. Clim.*, *12*, 1117–1133, 1999.

Severinghaus, J. P., Studies of terrestrial O_2 and carbon cycles in sand dune gases and in Biosphere 2, Ph.D. thesis, Columbia Univ., New York, 1995.

Shaffer, G., O. Leth, O. Ulloa, J. Bendtsen, G. Daneri, V. Dellarossa, S. Hormazabal, and P.-I. Sehlstedt, Warming and circulation change in the eastern South Pacific Ocean, *Geophys. Res. Lett.*, *27*, 1247–1250, 2000.

Siegenthaler, U., and H. Oeschger, Biospheric CO_2 emissions during the past 200 years reconstructed by convolution of ice core data, *Tellus, Ser. B*, *39*, 140–154, 1987.

Stocker, T. F., and A. Schmittner, Influence of CO_2 emission rates on the stability of the thermohaline circulation, *Nature*, *388*, 862–865, 1997.

Stocker, T. F., D. G. Wright, and L. A. Mysak, A zonally averaged, coupled ocean-atmosphere model for paleoclimate studies, *J. Clim.*, *5*, 773–797, 1992.

Tans, P. P., I. Y. Fung, and T. Takahashi, Observational constraints on the global atmospheric CO_2 budget, *Science*, *247*, 1431–1438, 1990.

Wanninkhof, R., Relationship between wind speed and gas exchange over the ocean, *J. Geophys. Res.*, *97*, 7373–7382, 1992.

Watanabe, Y. W., T. Ono, A. Shimamoto, T. Sugimoto, M. Wakita, and S. Watanabe, Probability of a reduction in the formation rate of the subsurface water in the North Pacific during the 1980s and 1990s, *Geophys. Res. Lett.*, *28*, 3289–3292, 2001.

Weiss, R. F., The solubility of nitrogen, oxygen and argon in water and seawater, *Deep Sea Res., Part II*, *17*, 721–735, 1970.

Wigley, T. M. L., A. K. Jain, F. Joos, B. S. Nyenzi, and P. R. Shukla, Implications of Proposed CO_2 Emissions Limitations, *Tech. Pap. IV*, 41 pp., Intergov. Panel on Clim. Change, Geneva, 1997.

Wright, D. G., and T. F. Stocker, Sensitivities of a zonally averaged global ocean circulation model, *J. Geophys. Res.*, *97*, 12,707–12,730, 1992.

F. Joos and T. F. Stocker, Climate and Environmental Physics, Physics Institute, University of Bern, Sidlerstrasse 5, CH-3012 Bern, Switzerland. (joos@climate.unibe.ch; stocker@climate.unibe.ch)

G. K. Plattner, Biogeochemistry Group, Institute of Geophysics and Planetary Physics, 5853 Slichter Hall, University of California, Los Angeles, Los Angeles, CA 90095-1567, USA. (plattner@igpp.ucla.edu)